J Mater Sci (2009) 44:1588–1593
DOI 10.1007/s10853-008-3232-7

Nanomechanical and surface behavior of polydimethylsiloxane-filled nanoporous anodic alumina

Te-Hua Fang · Tong Hong Wang · Shao-Hui Kang

Received: 10 October 2008 / Accepted: 29 December 2008 / Published online: 27 January 2009

Abstract In this article, the mechanical and wetting behavior of anodic aluminum oxide (AAO) and nanoporous-filled AAO were investigated using nanoindentation and contact angle measurements. The results showed that the nanoporous AAO was hydrophobic with a contact angle of 105°. The polymer filling affected the surface property and reduced the contact angle to 84°. The effects of the nanoporous filling on the Young's modulus and the hardness are investigated and discussed. A three-dimensional finite element model was also successfully developed to understand the nanoindentation-induced mechanism. A maximum von Mises stress of 1058 MPa occurred beneath the indenter.

Introduction

Nanoporous materials have attracted great attentions for their wide applications in the field of nanotechnology, such as catalysis, chemical/biosensors, templates for self-assembly, filters, nanofluidic transistors, and humidity sensors [1–3]. These materials can be produced by anodization techniques, which enable the fabrication of membranes with unique, well-defined nanopores.

The nanopores with size scales from 5 nm to 10 μm are strongly dependent on the voltage used for anodization. There are many membranes capable of achieving this nanoarchitecture. However, with regard to ease of fabrication with a wide variety of pore size, chemically and thermally stable and inert, nanoporous alumina (Al_2O_3) is the most appropriate candidate [4]. It has been shown that the modulus and hardness of nanoporous alumina varies with the pore size [5], and thus the pore size must be reduced if the strength of the material is a concern. However, this limits the use of relatively broad size pores, indicating that application breadth is restricted. Additionally, the pores have complicated geometries, and it is difficult to compare the actual wetting behavior with simple theoretical predictions.

In this article, we report on an enhanced nanoporous anodic aluminum oxide (AAO) filled with polydimethylsiloxane (PDMS), and compare the mechanical and wetting behavior of the nanoporous and nanoporous-filled AAO using experimental nanoindentation and contact angle measurements. Furthermore, three-dimensional finite element analyses (FEA) were conducted to explore the indentation response and mechanical properties of the AAO materials.

Experimental

Nanoporous AAO was prepared electrochemically using a two-step anodization technique to achieve oxide films with a regularly ordered porous structure. The first anodization was carried out until the residual Al film thickness approached the desired level, the oxides were then stripped away and subsequently the second anodization was performed until the remaining Al was completely anodized. A Ti sheet was used as a cathode for the anodization of the Al samples under a constant voltage. The first anodization was

T.-H. Fang (✉) · S.-H. Kang
Institute of Mechanical and Electromechanical Engineering, National Formosa University, Yunlin 632, Taiwan
e-mail: fang.tehua@msa.hinet.net

T. H. Wang
Thermal Laboratory, Advanced Semiconductor Engineering Inc, Kaohsiung 811, Taiwan

performed using a 0.4 M oxalic acid solution at 20 °C and 50 V for 4 h, and then the oxides were removed by immersing the samples in a mixture of 2 wt% chromic acid and 6 wt% phosphoric acid at a temperature of 60 °C. The desired thickness of the AAO films was obtained by subsequent second anodization. After the second anodization, the AAO could be widened by increasing the anodization time and the concentration of the acid solution.

For the pore-widening process, the solution used is 0.1 M phosphoric acid at a temperature of 30 °C for about 1 h. The filled AAO sample was fabricated by filling the recessed areas of the AAO via capillary forces. The PDMS was formed by curing Sylgard 184 siloxane prepolymer in a plastic Petri dish, pouring it into the AAO samples and then subsequently curing it at a temperature of 80 °C for 2 h.

Microstructure and surface properties of the AAO samples were measured using a scanning electron microscope (SEM, Hitachi S-3000N). The SEM was operated between 10 and 15 kV on samples containing an ultrathin layer of Pt coating. A nanoindentation device (Hysitron Triboscope) equipped with a Berkovich diamond probe with a radius of approximately 200 nm was used to measure the nanomechanical properties in the experiment. Three peak loads: 1, 3, and 5 mN were used for both nanoporous and nanoporous-filled AAO. To understand how the interfacial properties affect the introduction of water molecules on the AAO, the sessile drop method and the optical contact angle were used to estimate the wetting properties of a localized region on a solid surface. Deionized (DI) water droplets with a total volume of 5 μL were made for the subsequent contact measurement.

Results and discussion

Figure 1a shows the SEM image of the resultant AAO microstructure. The cylindrical open pores penetrated the entire thickness of the samples. The hole diameter of each pore was approximately 200 nm. Figure 1b shows the cross-sectioned view of the AAO. It can be seen that the discriminable pores are distributed macroscopically. Figure 1c shows the SEM image of the PDMS-filled AAO sample. The PDMS was filled into the pores of the AAO samples.

Contact angles have been used as a measure of wetting between a liquid and a solid surface [6]. Figure 2 shows the side views of the DI water droplet on the surface of the nanoporous and PDMS-filled AAOs. The contact angles for the nanoporous and the PDMS-filled AAO were 105° and 84°, respectively. Filling the pores increases the wettability of the nanoporous AAO. Organic materials like PDMS are considered as low-energy materials with respect to their surface energies, whereas inorganic materials like AAO are

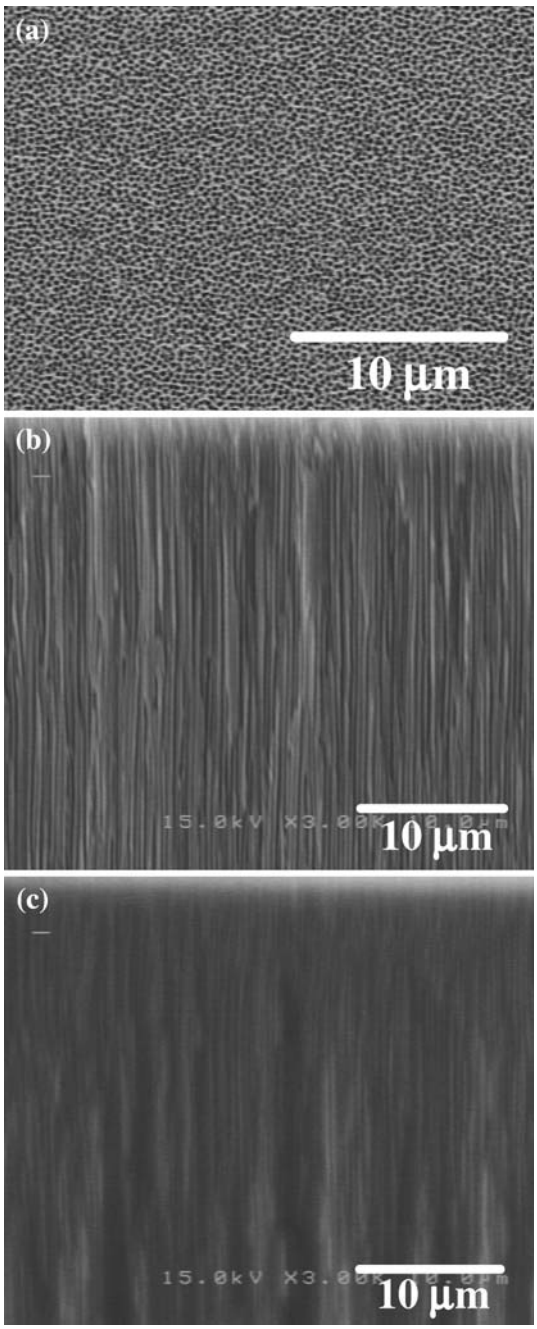

Fig. 1 SEM images of **a** the plan view of nanoporous AAO, **b** the cross-sectioned view of nanoporous AAO, and **c** nanoporous-filled AAO

referred to as high-energy materials. Therefore, either low- or high-energy liquids can be spread widely on coupled high- and low-energy surfaces like the PDMS-filled AAO sample.

Nanoindentation has been widely used for measuring nanomechanical properties such as the hardness and Young's modulus of samples [7]. Figure 3 shows the corresponding load–displacement (*L–D*) curves for different loads at room temperature. The overlapping loading curves

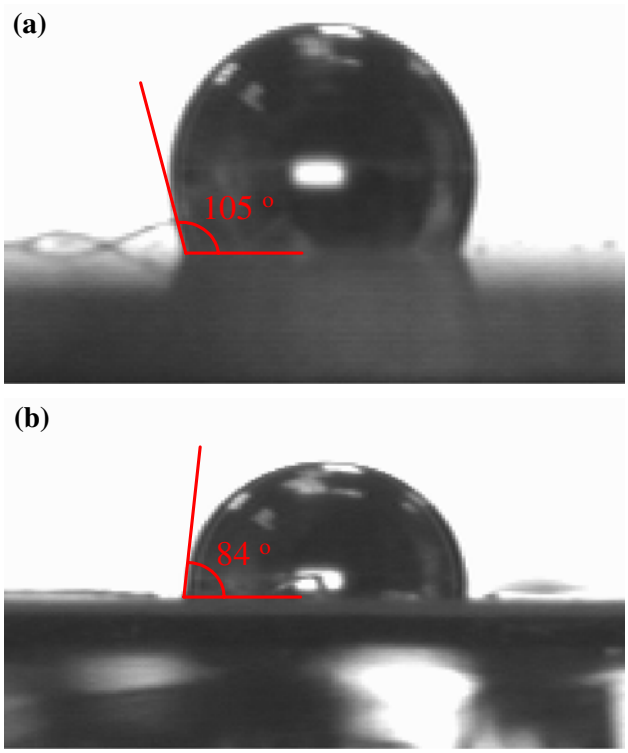

Fig. 2 Side view of the DI water drop on the **a** nanoporous and **b** nanoporous-filled AAOs

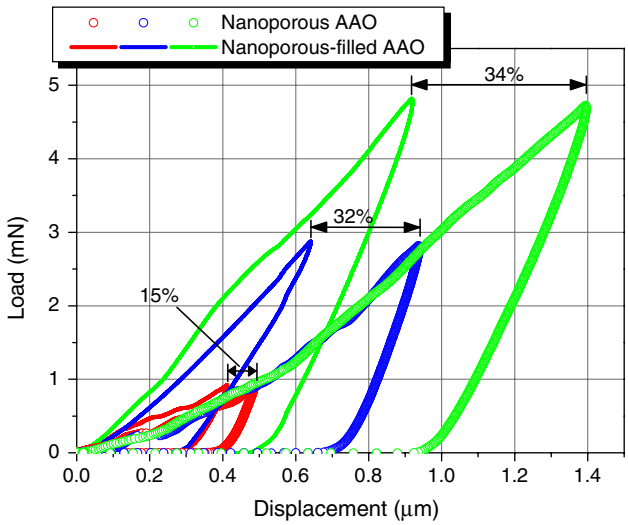

Fig. 3 *L–D* curves of the nanoporous and the nanoporous-filled AAO for different loads

of the nanoporous AAO exhibited excellent reproducibility of the indentation measurements. However, for the loading curves of the nanoporous-filled AAO, some discrepancies were found between samples. This may be due to the uncertain filling density of the PDMS-filled sample. At any rate, there were distinct differences between the nanoporous and the nanoporous-filled AAO sample. More importantly, it is evident from the results that the nanoporous-filled AAO had relatively shallow indentations when compared with those of nanoporous AAO, although the loads were identical. There were 15, 32, and 34% peak displacement reductions of the nanoporous-filled AAO at the peak loads of 1, 3, and 5 mN, respectively, compared to those of the nanoporous AAO. These results show that the strength of nanoporous-filled AAO was enhanced significantly after being filled with PDMS.

To further characterize the mechanical enhancements, we examined the hardness and Young's modulus of the samples. Hardness is defined as the resistance to local deformation. It is expressed as the maximum indentation load, $P_{\max}$, divided by the contact area, A,

$$H = \frac{P_{\max}}{A} = \frac{P_{\max}}{24.5h_c^2} \tag{1}$$

where the contact area is a function of contact depth, h_c, and the constant of 24.5 is used for a perfect Berkovich indenter tip. Young's modulus, E, of the test material can be obtained by the following equation [8],

$$E = (1-\nu^2)\left[\frac{1}{E^*} - \frac{1-\nu_i^2}{E_i}\right]^{-1} \tag{2}$$

where ν is the Poisson's ratio of the test material, while E_i and ν_i denote Young's modulus and Poisson's ratio of the indenter, respectively. The indenter properties used in this study are $E_i = 1140$ GPa and $\nu_i = 0.07$. E^* is the reduced modulus of the system and can further be defined as

$$E^* = \frac{\sqrt{\pi}}{2}\frac{S}{\beta\sqrt{A}} \tag{3}$$

where S is the stiffness of the test material, which can be determined from the slope of the initial unloading by evaluating the maximum load and the maximum depth, where $S = \mathrm{d}P/\mathrm{d}h$. β is a shape constant of the indenter, which is 1.034 for the Berkovich tip [9].

Figure 4a shows the hardness of the nanoporous and nanoporous-filled AAO samples. The hardness for the nanoporous AAO ranges between 0.16 and 0.18 GPa while those for the nanoporous-filled AAO between 0.46 and 0.61 GPa. Using hardness of the nanoporous AAO as the reference point, the hardness of the nanoporous-filled AAO enhances up to 206–245% in this particular study. This is to be expected, since the hardness is inversely proportional to the square of displacement, as in Eq. 1, and the shallower indentation incurs quadratic higher hardness if the loads are identical. This substantial improvement ensures the integrity of the structure, which is especially important for surface and coating applications.

Figure 4b shows the Young's moduli of the nanoporous and nanoporous-filled AAOs for different indentations. The comparatively high hardness of nanoporous-filled AAOs was matched by the high Young's moduli. The Young's

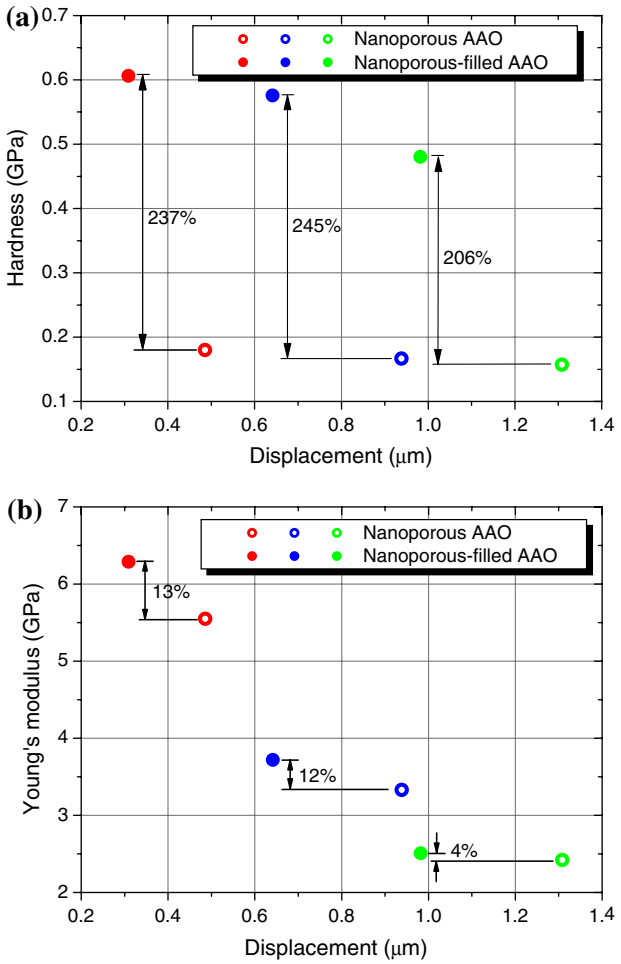

Fig. 4 **a** Hardness and **b** Young's moduli of the nanoporous and nanoporous-filled AAOs for different indentations

moduli of the nanoporous-filled AAOs showed higher values by factors in the range 4–13% with respect to the nanoporous AAOs. Moreover, the low modulus of the samples is probably associated with the absorbed moisture or residual water from the anodizing process [10]. It is also interesting to note that the hardness and Young's moduli demonstrated here were considerably lower than those found elsewhere [5], with the measured mechanical properties of the samples decreasing significantly as the pore diameter increases. This is because the pore diameter was larger than in the other study. The decrease in both hardness and Young's modulus are a combination of structural differences and mechanical effects [11].

Figure 5 shows the SEM image of an indented mark after nanoindentation. The indent mark for extended accuracy in the cross section was prior covered with Pt and then milled by the focused ion beam (FIB) milling technique. At this stage, the indent of the nanoporous AAO is shown as enclosed dash line. The porous structure leads to a deformation mechanism via crushing pores although the

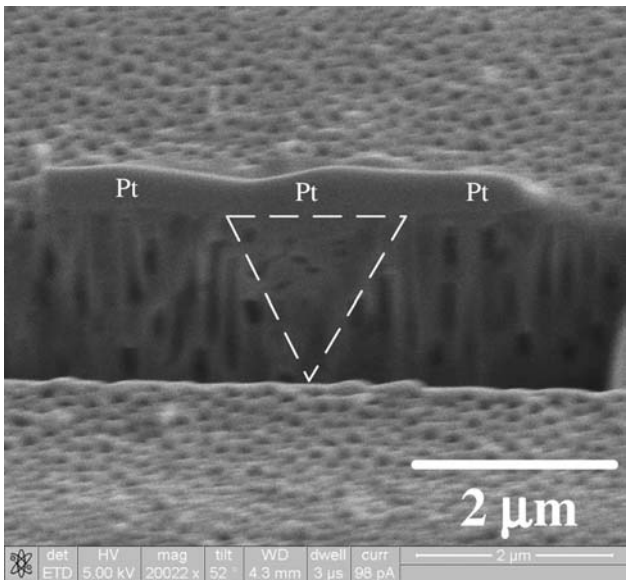

Fig. 5 SEM image of the AAO view through FIB technique. *Enclosed dash line* represents the indent mark covered by Pt

solid barrier layer did partially mitigate the crushing pores beneath the indenter.

A three-dimensional finite element model under the assumption of sixth symmetry was built to analyze the detailed mechanical behaviors. The AAO has a Young's modulus of 370 GPa, a yield stress of 260 MPa, a strain hardening exponent of 0.22, and a Poisson's ratio of 0.22 while the PDMS has a Young's modulus of 2 GPa, a yield stress of 100 MPa, a strain hardening exponent of 0.5, and a Poisson's ratio of 0.45 at room temperature. This way, the AAO and the PDMS behaved as plastically deformable solid. No properties inputted were required for the diamond Berkovich indenter since we treated it as rigid material. Here, we analyzed the nanoindentation of the nanoporous-filled AAO with the load of 3 mN; one of the load has been made of the experiments. The analysis is carried out using commercial finite element software ANSYS v 10.0.

Figure 6a shows the von Mises stress distributions of the nanoporous-filled AAO at the maximum load. During the maximum load, most of the von Mises stress distribution of the sample beneath the indenter exceeded its yield stress and gradually increased to a maximum near to the center, incurring the highest von Mises stress of 1058 MPa. The PDMS filling in the nanopores beneath the indenter, which was a relatively soft material, incurred lesser stress than the AAO, and had a maximum von Mises stress of 384 MPa, i.e., about one-third magnitude of the AAO bore. Nevertheless, for the PDMS filling away from where the indenter made contact, there was almost no stress generated, even at the maximum load. This revealed that for a nanoporous-filled AAO, AAO itself endured most of the indentation load, while the PDMS filling prevented from the

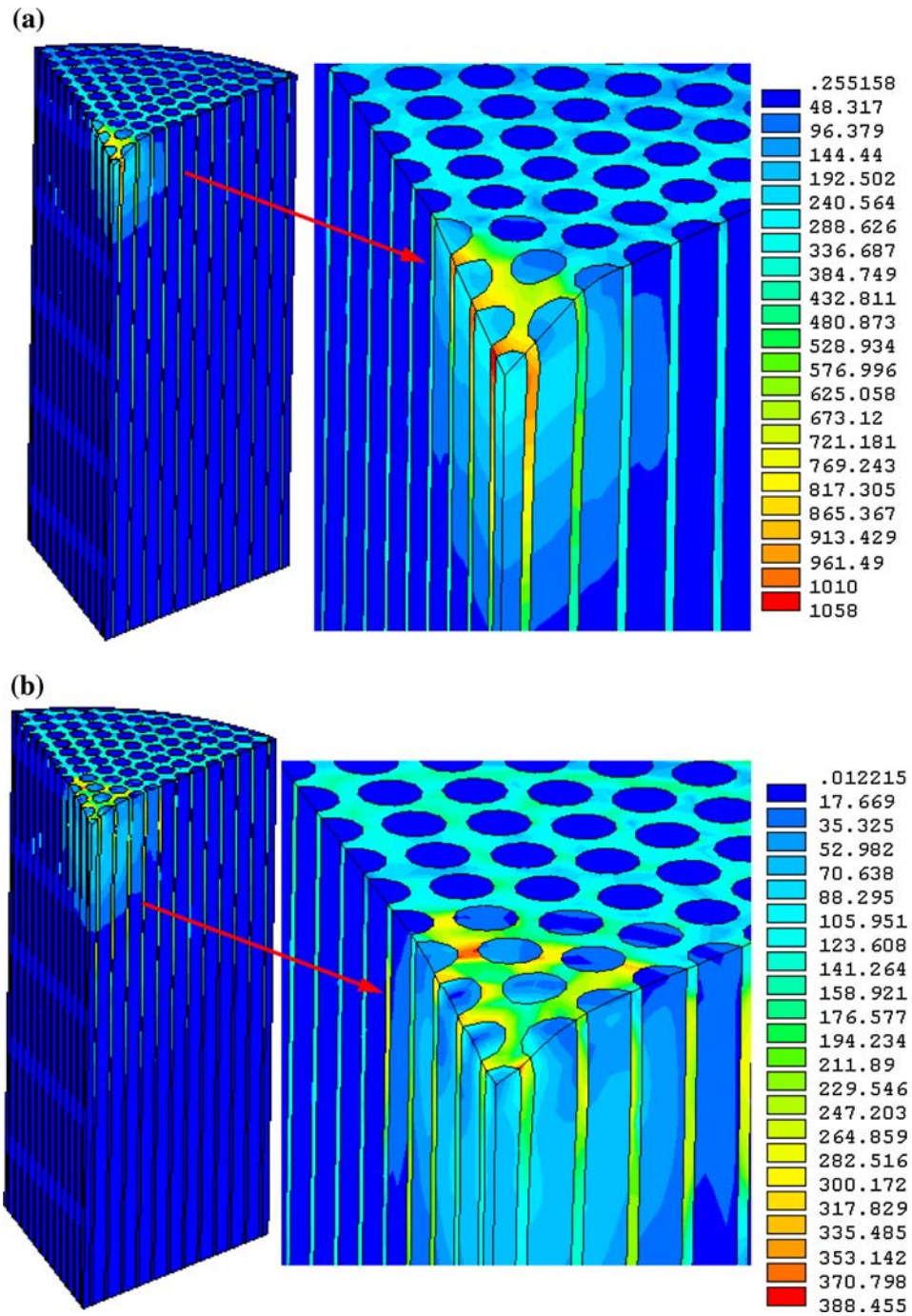

Fig. 6 Von Mises stress distributions of the nanoporous-filled AAO during maximum load (Unit: MPa)

deformation only at those areas beneath the indenter. In other words, filling the nanopores does help to restrain the indentation displacement. Figure 6b shows the von Mises stress distributions of the nanoporous-filled AAO after unload. Obviously, the AAO rebound a little bit and remain a residual maximum von Mises stress of 389 MPa. Compared to maximum load, the stress distributions are similar. This qualitative approach successfully describes the interaction mechanism between nanopores and PDMS.

Conclusion

In summary, we have demonstrated the mechanical and wetting behaviors of nanoporous and nanoporous-filled AAOs. Although the fabricated pore diameter, reported here, is larger than in other literatures, the hardness and Young modulus of the nanoporous-filled AAO are obviously and slightly enhanced when compared to the standard nanoporous AAO. The wetting behavior is also improved

by filling the AAO structures with PDMS. Finite element analysis on nanoporous-filled AAO reveals that AAO itself endures most of the indentation load, while the PDMS filling prevents from the deformation only at those areas beneath the indenter which do help to restrain the indentation displacement.

Acknowledgement This work was supported in part by the National Science Council of Taiwan under Grant No. NSC95-2221-E150-066.

References

1. Benfield RE, Grandjean D, Kroll M, Pugin R, Sawitowski T, Schmid G (2001) J Phys Chem B 105:1961
2. Yang H, Rahman S (2003) Nano Lett 3:439
3. Varghese OK, Gong D, Paulose M, Ong KG, Grimes CA, Dickey EC (2002) J Mater Res 17:1162
4. Popat KC, Mor G, Grimes CA, Desai TA (2004) Langmuir 20:8035
5. Ko S, Lee D, Jee S, Park H, Lee K, Hwang W (2006) Thin Solid Films 515:1932
6. Redon R, Vazquez-Olmos A, Mata-Zamora ME, Ordonez-Medrano A, Rivera-Torres F, Saniger JM (2006) Rev Adv Mater Sci 11:79
7. Fang TH, Chang WJ (2003) Microelectron Eng 65:231
8. Fang TH, Chang WJ (2006) Appl Surf Sci 252:6243
9. Wang TH, Fang TH, Lin YC (2007) Appl Phys A 86:335
10. Grosskreutz JC (1969) J Electrochem Soc 116:1232
11. Wang TH, Fang TH, Lin YC (2007) Mater Sci Eng A 447:244